JOURNAL OF GUIDANCE, CONTROL, AND DYNAMICS
Vol. 30, No. 6, November–December 2007

Closed-Form Specified-Fuel Commands for Two Flexible Modes

Yoon-Gyung Sung*
Chosun University, Gwangju 501-759, South Korea
and
William E. Singhose†
Georgia Institute of Technology, Atlanta, Georgia 30332

DOI: 10.2514/1.29954

A method is proposed for generating on–off commands for rest-to-rest slewing of two-mode systems. When the on–off actuators are thruster jets, the command profiles can be designed to use a specified amount of fuel. When the on–off actuators are motors or valves, the method can accommodate a specified velocity limit. A benefit of the procedure is that it uses closed-form functions of the system parameters and desired maneuver. The performance of the commands is evaluated in terms of slewing speed, maximum transient deflection, and robustness to system uncertainty. The proposed method is demonstrated with a numerical simulation of a benchmark two-mode spacecraft model and experimentally validated on a bridge crane exhibiting double-pendulum dynamics.

I. Introduction

DISCONTINUITY of on–off commands can induce large transient and residual vibration in flexible systems. Both low and high modes can be excited by the aggressive forcing function. This phenomenon has been investigated in spacecraft actuated by on–off thruster jets [1–4]. These potentially adverse effects have motivated many approaches to create on–off commands that reduce residual vibration in multimode flexible systems [1,5–8].

One drawback to many of the proposed on–off command-generation schemes is that they rely on using numerical optimization that can be difficult to implement in real time. Furthermore, the optimized solutions may use a significant amount of actuator fuel that is expensive to carry into space. To reduce fuel consumption, previous methods have produced fuel-minimum profiles [9], fuel-efficient [10], specified-fuel [11], and fuel/time-optimal commands [12–14].

Recently, some practical advancements based on input shaping [15] have been made by considering robustness [16], limitation of transient deflection [17], and fuel consumption [10]. Closed-form (CF) methods [18,19] have been developed to avoid numerical-optimization-based approaches that may be difficult to implement. However, the previous closed-form methods concentrated on suppressing only one dominant mode. This paper proposes an advanced procedure to eliminate two flexible modes while allowing specified fuel usage or enforcing a fixed velocity limit.

To develop closed-form on–off commands for two-mode systems, the commands are designed using a three-step procedure. The first phase accelerates the system from rest without inducing vibration. The second phase is a coasting period in which the system is moving with zero vibration. The last phase decelerates the system back to rest without inducing residual vibration. A schematic representation of the proposed commands is shown in Fig. 1. This command profile will not result in a time-optimal command. Time-optimal commands generally switch between full positive and full negative actuator effort and require a numerical optimization to obtain their switch times. The proposed profile is used so that a closed-form solution can be obtained.

The next section presents a method that generates on–off commands that are parameterized by move distance, fuel usage, mode ratio, and force-to-mass ratio. Then, a performance evaluation is presented with respect to move distance, fuel usage, and mode ratio with a benchmark two-mode system. Finally, the performance of the proposed method is validated by experiments on a bridge crane that exhibits double-pendulum dynamics.

II. Development of Two-Mode Closed-Form Commands

The command-generation procedure proposed here is based on input-shaping concepts [15] and transition shaping [18]. Input shaping is a notch-filtering technique, whereby a specially designed sequence of impulses, known as the input shaper, is convolved with a reference command to form a new command that causes little or no residual vibration. Figure 2 shows that convolving a step function with a sequence of ± 1 impulses will produce a sequence of positive on–off pulses that can accelerate a flexible system with zero residual vibration, provided that the correct impulse times are used. To decelerate the system, the antisymmetrical negative pulse sequence is used. The command profile developed by this method can be an attractive alternative to time/fuel-optimal commands [13,14].

The entire duration of the command pulses must be constrained to consume the desired amount of actuator fuel (or observe the velocity limit) during a maneuver. This requires

$$-t_1 + t_2 - t_3 + t_4 \cdots - t_{k/2-1} + t_{k/2} \leq \frac{U}{2} \tag{1}$$

where U is the desired fuel usage in seconds, and k is the number of command switches in the command profile (acceleration and deceleration). If Eq. (1) is used in conjunction with input-shaping constraint equations, then a proper acceleration profile can be

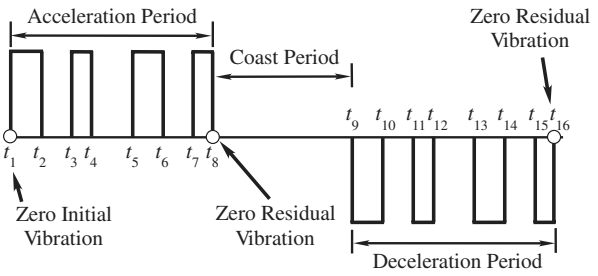

Fig. 1 Proposed on–off pulse command profile.

Received 23 January 2007; revision received 5 June 2007; accepted for publication 7 June 2007.

*Associate Professor, Department of Mechanical Engineering; sungyg@chosun.ac.kr.

†Associate Professor, Woodruff School of Mechanical Engineering; singhose@gatech.edu.

determined. Note that this problem formulation is equivalent to specifying a maximum velocity; therefore, the technique in this paper is also useful for velocity-limited systems such as the crane used in the experimental validation.

For oscillatory modes, the constraint to ensure zero vibration (ZV) of an undamped system is given by the following equation:

$$\sqrt{\left[\sum_{i=1}^{n} A_i \cos(\omega_j t_i)\right]^2 + \left[\sum_{i=1}^{n} A_i \sin(\omega_j t_i)\right]^2} = 0 \qquad (2)$$

where A_i and t_i are the amplitudes and time locations of the impulses, and ω_j is the natural frequency of the system's jth mode. By introducing additional constraints [15,16], more robust commands can be obtained. However, ZV commands will only be considered here, to focus on controlling fuel usage in conjunction with two-mode vibration suppression.

To satisfy the ZV constraints (2) and the fuel-consumption requirement (1), four acceleration pulses are used, as shown in Fig. 2. By assuming that the time of the first impulse t_1 is equal to zero, there remain only seven unknown impulse-time locations that must be determined. Given a mode ratio of $r = \omega_2/\omega_1 > 1$, the pulse sequence can be determined in closed form by assigning a specific role to each impulse in terms of inducing or canceling vibration. As shown in Fig. 3, the positive impulses during the acceleration phase can be designed to produce zero vibration in both modes. The impulse at t_3 cancels the second-mode vibration induced by the impulse at t_1. Then the impulses at t_5 and t_7 cancel the first-mode vibration of the impulses at t_1 and t_3. Because the time spacing between t_5 and t_7 is the same as that between t_1 and t_3, the vibration of both the first and second modes is canceled by the four impulses. The time spacings of the negative impulses used to form the on–off pulses are the same as those of the positive impulses, except they are shifted over in time to obtain the eight impulses shown in Fig. 2.

The second-mode vibration caused by the impulse at t_1 can be canceled if t_3 is an odd multiple of $T_2/2$, where T_2 is the period of ω_2:

$$t_3 = (2m+1)\frac{T_2}{2} \qquad (3)$$

where $m = 0, 1, 2, \ldots$. When t_3 is chosen according to Eq. (3), only the first-mode vibration will exist between t_3 and t_5, as shown in Fig. 3. If t_5 is placed at an odd multiple of $T_1/2$, where T_1 is the period of ω_1, then the first-mode vibration induced by the impulse at t_1 will be canceled by the impulse at t_5:

$$t_5 = (2n+1)\frac{T_1}{2} \qquad (4)$$

where $n = 0, 1, 2, \ldots$. For t_7 to cancel the second-mode vibration induced by t_5, it must be

$$t_7 = t_5 + t_3 \qquad (5)$$

The negative impulses at t_2, t_4, t_6, and t_8 have the same relative time separation as the positive impulses at t_1, t_3, t_5, and t_7. However, they are shifted in time to satisfy the fuel-usage constraint. This is accomplished if the shift is set equal to $U/8$. In this case, the four pulses in the acceleration phase will use half of the allotted fuel. The remaining fuel is used to decelerate the system to rest. To eliminate any pulse overlap, the following inequality is enforced:

$$t_2 < t_3 \quad \text{and} \quad t_4 < t_5 \qquad (6)$$

Solving for the possible range of fuel usage given any values of m and n while minimizing t_8 yields

$$U < 4(2n+1)T_1 + 4(2m+1)T_2 \qquad (7)$$

The values of m and n for any amount of fuel usage can be obtained by using the inequality in Eq. (7). Once m and n are known, the impulse times that generate the acceleration pulses can be computed as

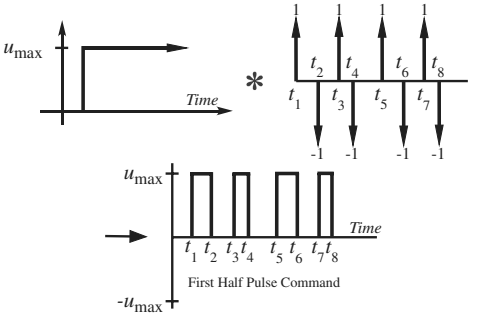

Fig. 2 Convolution to create on–off pulses.

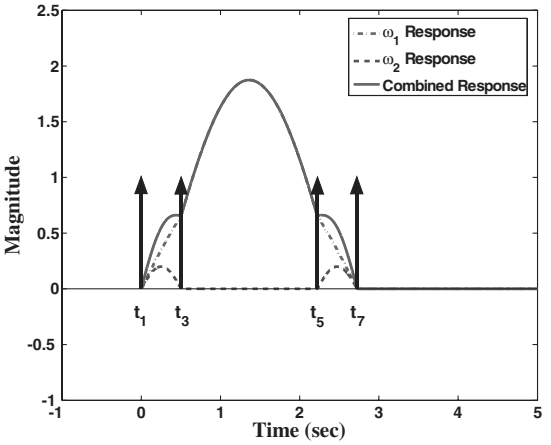

Fig. 3 Two-mode vibration cancellation process.

$$\begin{aligned} &t_1 = 0 \quad t_2 = U/8 \quad t_3 = (2m+1)T_2/2 \quad t_4 = t_3 + U/8 \\ &t_5 = (2n+1)T_1/2 \quad t_6 = t_5 + U/8 \quad t_7 = t_5 + t_3 \\ &t_8 = t_5 + t_3 + U/8 \end{aligned} \qquad (8)$$

Equation (8) gives the on–off switch times of a four-pulse command for accelerating without producing residual vibration in two flexible modes.

The duration of the coast period between acceleration and deceleration must be determined by considering the rigid-body mechanics. The midpoint time of a maneuver is expressed by

$$t_m = \frac{(t_8 + t_9)}{2} \qquad (9)$$

where t_9 is the time at which the deceleration pulses begin, as shown in Fig. 1. If a system has total mass M and the position of the system's center of mass is x, then the equation describing rigid-body motion is expressed by

$$\ddot{x}(t) = u(t)/M \qquad (10)$$

The on–off forcing function $u(t)$ can be expressed as

$$u(t) = 1 + \sum_{i=2}^{8} (-1)^{(i+1)} \mathcal{H}(t - t_i) \qquad (11)$$

where $\mathcal{H}$ denotes the Heaviside function. If the system starts from a state of rest, then it is easy to obtain the position of the system's mass center by integrating Eq. (10) twice. Given the simple form of the control profile given in Eq. (11), the integration can be determined in closed form. When we set the double integral equal to one-half of the desired distance x_d at the midpoint of the maneuver, we obtain

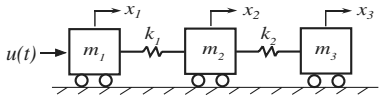

Fig. 4 System with two oscillation modes.

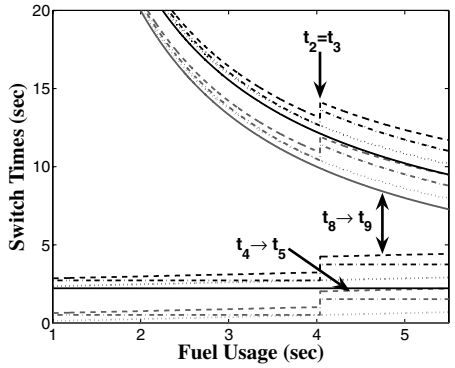

Fig. 5 Switch times with respect to fuel usage.

$$x_d/2 = \alpha\left(-t_2^2 + t_3^2 - t_4^2 + t_5^2 - t_6^2 + t_7^2 - t_8^2\right)/2 + \alpha(t_2 - t_3 + t_4 - t_5 + t_6 - t_7 + t_8)t_m \tag{12}$$

where α is the force-to-mass ratio. Substituting Eqs. (9) into Eq. (12) and solving Eq. (12) with Eq. (8) for t_9 gives

$$t_9 = \frac{2x_d}{\alpha U} \tag{13}$$

Therefore, the switch times for the deceleration command are obtained in closed form:

$$\begin{aligned} &t_9 = 2x_d/(\alpha U) \qquad t_{10} = t_9 + t_2 \qquad t_{11} = t_9 + t_3 \\ &t_{12} = t_9 + t_4 \qquad t_{13} = t_9 + t_5 \qquad t_{14} = t_9 + t_6 \\ &t_{15} = t_9 + t_7 \qquad t_{16} = t_9 + t_8 \end{aligned} \tag{14}$$

The entire closed-form command is described by Eqs. (8) and (14).

When commands are generated for the benchmark system with two oscillation modes (shown in Fig. 4), the switch times display a predictable dependence on the fuel usage. This effect is shown in Fig. 5 for the case when $\omega_1 = \sqrt{2}$ rad/s, $\alpha = 0.5$, $r = 4.4$, and $x_d = 20$ units. As the fuel usage increases, the values of t_2 and t_4 increase linearly. When t_2 equals t_3, the value of m in Eq. (10) increases by one and the switch time of t_3 jumps to 1.5 vibration periods of the second mode. Note that this causes a discontinuous increase in the command duration. Figure 5 shows that t_8 and t_9 continually approach each other as the fuel usage increases. After they become equal, additional fuel cannot be used, because the desired fuel usage (measured in seconds) exceeds the maneuver time. High levels of fuel usage provide only a marginal improvement in speed. In fact, most realistic cases of fuel usage on spacecraft would use relatively long coast durations between the acceleration period and the deceleration period.

III. Evaluation of Command Profiles

To compare the proposed commands against a baseline, a bang-coast-bang (BCB) command is employed. If we assume that the bang-coast-bang command begins at $t_1 = 0$, then the positive pulse for the acceleration from rest is ended at time $t_2 = U/2$. The negative pulse for the deceleration to rest is started at time t_3, which can be determined from the rigid-body dynamics. The entire BCB command is described by

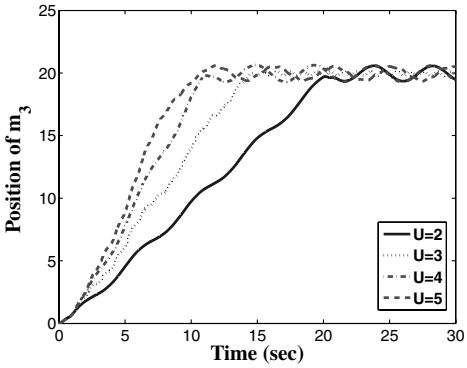

Fig. 6 Position responses of the third mass when driven by BCB commands.

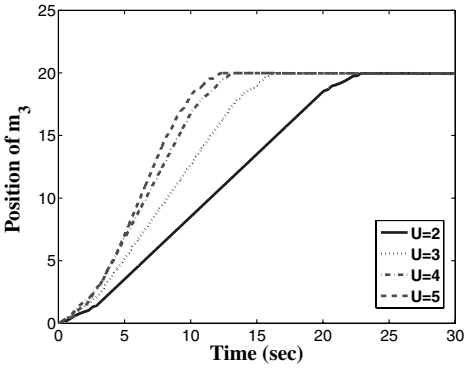

Fig. 7 Position responses of the third mass when driven by closed-form commands.

$$\begin{bmatrix} A_i \\ t_i \end{bmatrix} = \begin{bmatrix} 1 & -1 & -1 & 1 \\ 0 & \frac{U}{2} & \frac{2x_d}{\alpha U} & \frac{2x_d}{\alpha U} + \frac{U}{2} \end{bmatrix} \tag{15}$$

where x_d, α, A_i, and t_i are defined the same as in the previous section. The BCB command moves the center of mass to the desired position; however, significant residual vibration can be expected when it is applied to flexible systems.

Both the CF command and the BCB command were evaluated on the benchmark undamped two-mode system shown in Fig. 4. The first mode, $\omega_1 = \sqrt{2}$ rad/s, and the force-to-mass ratio, $\alpha = 0.5$, were fixed and the rest of the parameters, such as move distance x_d, fuel usage U, and mode ratio r, were varied to make performance comparisons.

Figure 6 shows the time response of the third mass when the system is driven by BCB commands. The BCB commands produce oscillation during the transient period and residual vibration after the end of the move for all levels of fuel usage. In contrast, Fig. 7 shows that the CF commands produce no visible oscillation during the coast period and no residual vibration after the desired move distance is achieved.

A. Dependence on Move Distance

To evaluate the performance as a function of move distance, the fuel usage ($U = 5$ s) and the mode ratio ($r = 4.4$) were fixed, and then move duration, maximum deflection, and insensitivity were evaluated as the move distance x_d was varied. Figure 8 shows the move duration as a function of the move distance. As expected, the BCB command is about 2 s faster than the CF command throughout all of the move distances. This small drawback of the CF command is compensated by superior performances in the other performance measures. After all, a small difference in maneuver time is not an important issue in flexible spacecraft when compared with vibration reduction and fuel usage.

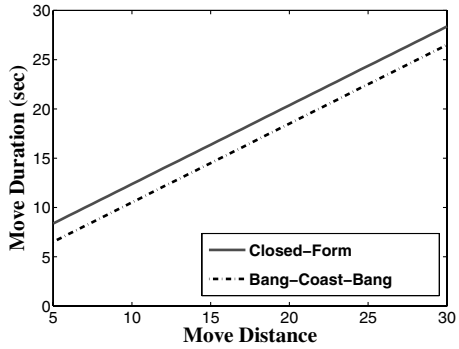

Fig. 8 Move duration vs move distance.

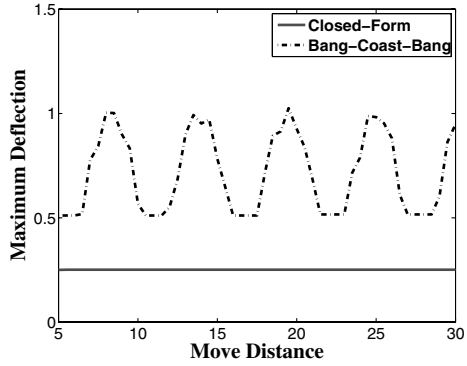

Fig. 9 Maximum deflection vs move distance.

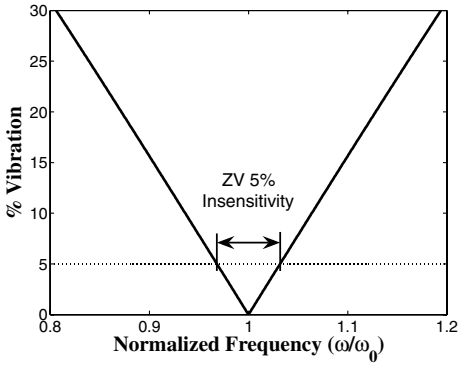

Fig. 10 Illustration of 5% insensitivity.

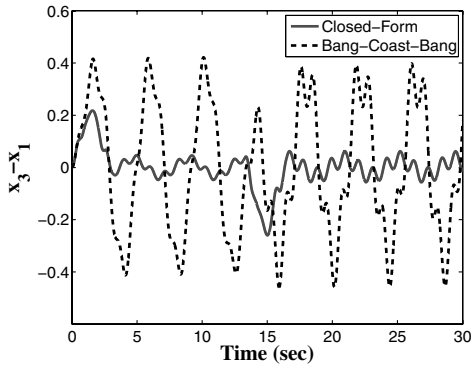

Fig. 11 Deflection of the third mass with 5% mode error.

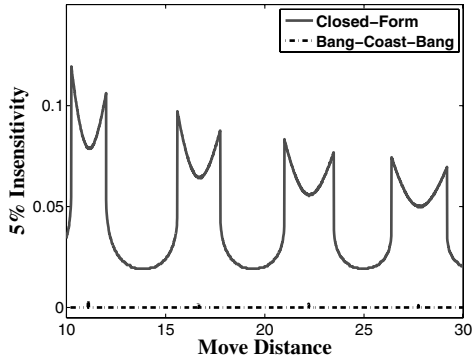

Fig. 12 First-mode 5% insensitivity vs move distance.

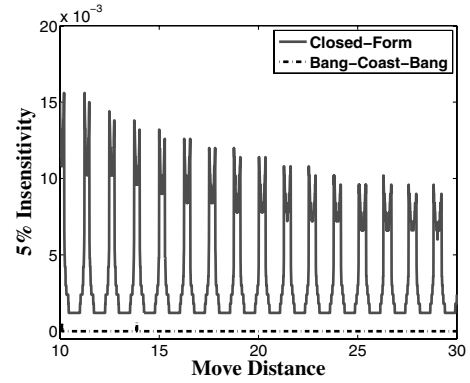

Fig. 13 Second-mode 5% insensitivity vs move distance.

A very important performance measure is the transient deflection of the system, because it can be associated with the lifetime of space structures. In fact, large deflection may cause critical damage to structures. Figure 9 shows the maximum transient deflection of the mass, m_3, as a function of move distance. The CF commands average 70% less deflection than the BCB commands. An interesting feature is that the deflection induced by the CF commands is constant for the entire range of the move distances.

Because of modeling errors or uncertainty in the flexible modes, robustness is another important measure. A sensitivity curve presenting the vibration amplitude resulting from modeling errors is shown in Fig. 10. The horizontal axis indicates the degree of modeling error by showing the actual frequency ω divided by the modeled frequency ω_0. The width of the curve that lies below a tolerable vibration level is defined as the insensitivity to the normalized frequency errors. The 5% insensitivity indicates what frequency range will have vibration below 5% of the vibration induced by a step input. For example, Fig. 11 shows the time response of the deflection between mass 3 and mass 1, $x_3 - x_1$, when there are errors of $+5\%$ in ω_1 and -5% in ω_2. The other parameters are the same as in Figs. 6 and 7, with $U = 3$ s, $\alpha = 0.5$, $r = 4.4$, and $x_d = 20$ units. Even with these modeling errors, the BCB command has two times more transient deflection and four times more residual vibration than the CF command.

The 5% insensitivity as a function of the move distance is shown in Fig. 12 for the first mode and in Fig. 13 for the second mode. The CF command has much better robustness than the BCB command. This is obvious, because the BCB command is not designed to suppress vibration.

B. Dependence on Fuel Usage

To appraise the effect of fuel usage, the move distance ($x_d = 10$ units) and the mode ratio ($r = 4.4$) were fixed, and then move duration, maximum deflection, and insensitivity were evaluated with the variation of the fuel usage U. The BCB commands are 2 to 3 s faster throughout the range of fuel usage shown in Fig. 14.

Figure 15 shows the maximum transient deflection of the mass m_3 as a function of fuel usage. The BCB commands produce larger

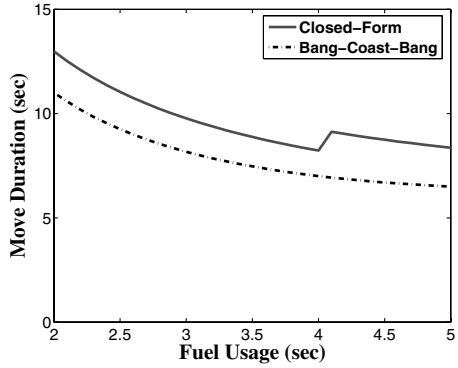

Fig. 14 Move duration vs fuel usage.

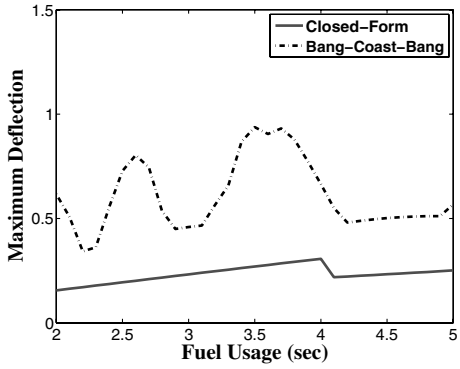

Fig. 15 Maximum deflection vs fuel usage.

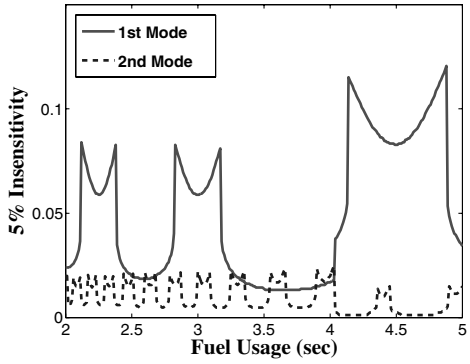

Fig. 16 Insensitivity of 5% of CF command vs fuel usage.

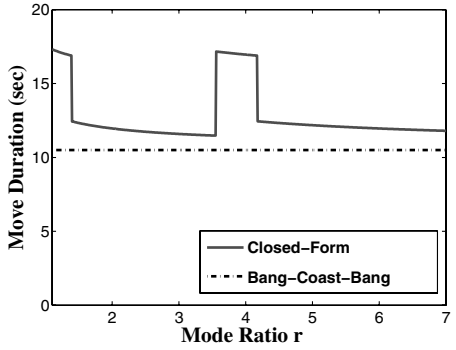

Fig. 17 Move duration vs the mode ratio.

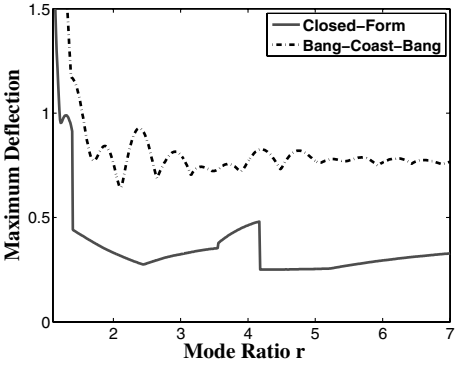

Fig. 18 Maximum deflection vs the mode ratio.

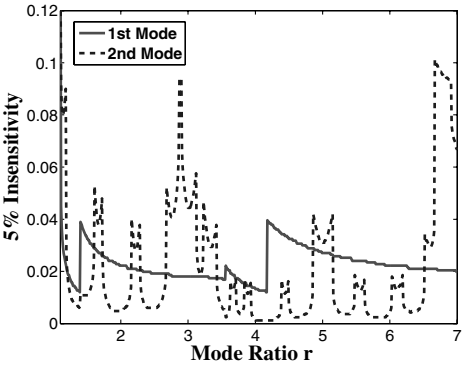

Fig. 19 Insensitivity of 5% of CF command vs the mode ratio.

transient deflection than do the CF commands. The deflection induced by the BCB commands varies substantially with fuel usage. The plot shows that the deflection magnitude of the CF commands drops slightly after 4 s.

Figure 16 shows the 5% insensitivity for the first and second modes. Only the CF commands are shown, because the BCB commands showed virtually zero insensitivity, such as in the previous evaluation with move distance. For the CF commands, the 5% insensitivity for the first mode gets wider and taller as fuel usage increases, whereas second-mode robustness decreases after a fuel usage of 4 s. Therefore, the second mode must be more carefully modeled when large amounts of fuel are used or, equivalently, the maximum velocity is increased.

C. Dependence on Mode Ratio

For the evaluation as a function of the mode ratio, the move distance ($x_d = 10$ units) and the fuel usage ($U = 5$ s) were fixed, and then move duration, maximum deflection, and insensitivity were evaluated. As shown in Fig. 17, the BCB commands are not dependent on the mode ratio. However, the CF commands do vary with mode ratios. The CF commands average 25% longer than the BCB commands over the range shown.

Figure 18 shows the maximum transient deflection of the mass m_3 as a function of the mode ratio. The BCB commands produce considerably more deflection than the CF commands. Except for small mode ratios, the deflection magnitude is not strongly dependent on the mode ratio. This is because the low mode dominates the response. Figure 19 shows the 5% insensitivity of the CF command. The second mode shows more robustness than the first mode for certain mode ratios.

IV. Experimental Results

Experimental tests were performed using a 10-ton industrial bridge crane at Georgia Tech, shown in Fig. 20. Its work space is 6.2 m high, 5 m wide, and 42 m long. Figure 21 shows a schematic diagram of the crane equipped with an advanced control system. A Siemens programmable logic controller (PLC) is connected to a laptop computer by a wireless local area network to perform the

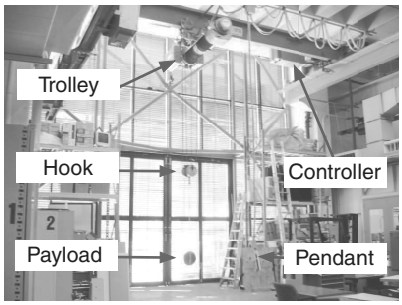

Fig. 20 Georgia Tech's 10-ton bridge crane.

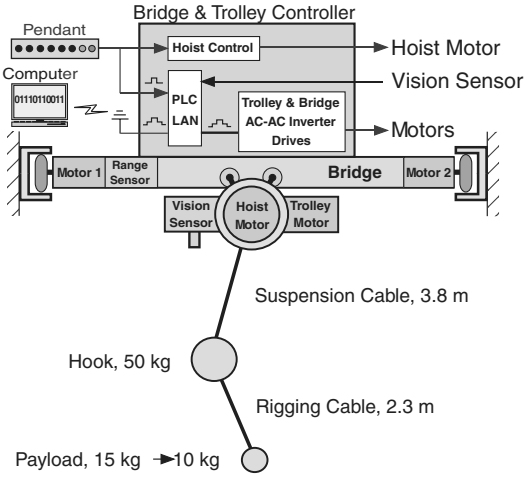

Fig. 21 Hardware configuration.

proposed algorithms. The velocity commands generated by the PLC are then sent to the trolley/bridge motor drives. The drives use the incoming commands from the PLC as velocity set points for the motors. To ensure accurate execution of the commands, the trolley/bridge control system has Siemens Masterdrives Series AC-AC inverters, which use a pulse-width-modulated signal to accurately control the inverter-duty-capable motors. For accurate measurements, the control system has a laser range sensor and a Siemens machine vision system.

A double pendulum was formed by attaching a payload to the hook of the crane with a rigging cable. The length of the suspension cable was approximately 3.8 m and the rigging length was approximately 2.3 m. The mass of the hook was approximately 50 kg and the mass of the payload was 15 kg. With this setup, the natural frequencies are $\omega_1 = 1.45$ rad/s and $\omega_2 = 2.61$ rad/s. Note that the crane has numerous other vibration modes throughout its structure. For example, the overhead trolley will rock back and forth about its connection to the bridge. The bridge is a 9-m-long I-beam that must support the trolley, and so it deflects under the weight and motion of the trolley. However, these modes do not contribute in a significant way to the payload oscillation. In fact, their effects cannot normally be seen or measured in the payload response. Therefore, this experimental setup provides a very good testbed for control of two-mode systems.

Crane operation is based on velocity commands; therefore, the proposed input commands were converted into velocity commands, with the maximum velocity set to 0.339 m/s. The maximum acceleration was 0.678 m/s^2 and a sampling time of 35 ms was used. In each experiment, only the hook oscillation was measured by the overhead camera, because the camera view of the payload is periodically blocked by the swinging hook. However, the payload motion affects the response of the hook, and so the two-mode dynamics are detectable in the hook response. For the experimental demonstration, the fuel usage ($U = 2$ s) was fixed and the time response, residual oscillation with robustness, and maximum deflection were evaluated.

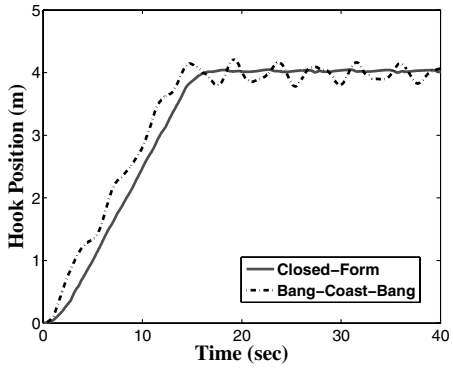

Fig. 22 Experimental time responses of the crane hook.

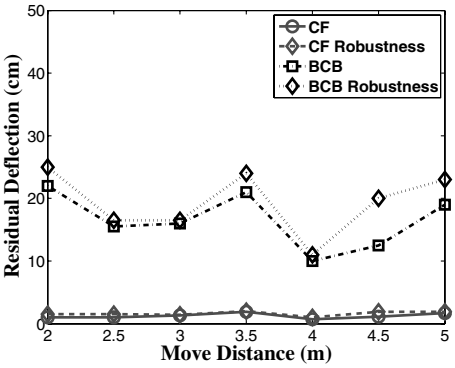

Fig. 23 Maximum oscillation of the crane hook with altered payload.

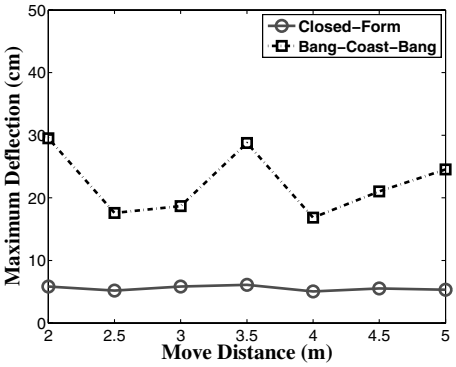

Fig. 24 Maximum deflection of the crane hook vs move distance.

Figure 22 shows that the CF command is vastly better than the BCB command for a 4-m move distance of the trolley. The CF command induces only small vibration magnitudes both during motion and after arriving at the target location. The BCB command does arrive at the target distance about 3 s faster. However, the BCB command has overshoot at the target distance and multimode residual vibration that takes several minutes to damp out.

Figure 23 illustrates the control robustness by showing the residual oscillation amplitude at the end of each command for seven different move distances. In these experiments, the weight of the payload was changed from 15 to 10 kg, and so ω_1 and ω_2 changed by $+2$ and -5%, respectively. The CF commands have an average increase of only 0.3 cm of residual oscillation. On the other hand, the BCB commands have large residual oscillation and an average increase of 2.8 cm. When the residual vibration magnitude of the crane hook is closely examined, the CF commands induce less than 1.5 cm over the range tested, and the BCB commands produced an average oscillation amplitude of 16.5 cm. Therefore, the CF commands showed good robustness when the system parameters and move distance were varied.

Figure 24 shows the maximum transient deflection as a function of the move distance. As expected from the theoretical evaluation, the CF commands produce less deflection (an average of 6 cm) than the BCB commands (an average of 23 cm). The CF commands produce nearly a constant maximum deflection for the entire operational range. This is because the maximum deflection of the CF commands occurs at the periods of accelerations and decelerations. On the other hand, the BCB commands shows large variation in deflection magnitudes, ranging from about 18 to 30 cm. These variations result from the dynamic beating phenomenon that causes the payload to excite the hook motion.

V. Conclusions

A closed-form method for generating on–off commands for two-mode systems was proposed. The commands were designed to accelerate and decelerate a system with two flexible modes without residual vibration when a desired amount of actuator fuel or a velocity limit was specified. The proposed closed-form commands cause low levels of transient deflection and have robustness to modeling errors. A significant advantage of the proposed method is that the on–off command is given in closed form. There is no need to perform a numerical optimization for every possible move distance and/or fuel usage. The closed-form on–off commands were validated by both numerical and experimental implementations.

Acknowledgments

This study was supported (in part) by research funds from Chosun University. In addition, the authors are grateful to Siemens Energy and Automation for their contribution to the development of the advanced bridge crane.

References

[1] VanderVelde, W., and He, J., "Design of Space Structure Control Systems Using On–Off Thrusters," *Journal of Guidance, Control, and Dynamics*, Vol. 6, No. 1, 1983, pp. 53–60.

[2] Farrenkopf, R. L., "Optimal Open-Loop Maneuver Profiles for Flexible Spacecraft," *Journal of Guidance and Control*, Vol. 2, No. 6, 1979, pp. 491–498.

[3] Swigert, C. J., "Shaped Torque Techniques," *Journal of Guidance and Control*, Vol. 3, No. 5, 1980, pp. 460–467.

[4] Turner, J. D., and Junkins, J. L., "Optimal Large-Angle Single-Axis Rotational Maneuvers of Flexible Spacecraft," *Journal of Guidance and Control*, Vol. 3, No. 6, 1980, pp. 578–585.

[5] Singh, T., and Vadali, S. R., "Robust Time-Optimal Control: A Frequency Domain Approach," *Journal of Guidance, Control, and Dynamics*, Vol. 17, 1994, pp. 346–353.

[6] Liu, Q., and Wie, B., "Robust Time-Optimal Control of Uncertain Flexible Spacecraft," *Journal of Guidance, Control, and Dynamics*, Vol. 15, No. 3, 1992, pp. 597–604.

[7] Ben-Asher, J., Burns, J. A., and Cliff, E. M., "Time-Optimal Slewing of Flexible Spacecraft," *Journal of Guidance, Control, and Dynamics*, Vol. 15, 1992, pp. 360–67.

[8] Singh, G., Kabamba, P. T., and McClamroch, N. H., "Planar, Time-Optimal, Rest-to-Rest Slewing Maneuvers of Flexible Spacecraft," *Journal of Guidance, Control, and Dynamics*, Vol. 12, 1989, pp. 71–81.

[9] Meyer, J. L., and Silverberg, L., "Fuel Optimal Propulsive Maneuver of an Experimental Structure Exhibiting Spacelike Dynamics," *Journal of Guidance, Control, and Dynamics*, Vol. 19, No. 1, 1996, pp. 141–9.

[10] Singhose, W., Bohlke, K., and Seering, W., "Fuel-Efficient Pulse Command Profiles for Flexible Spacecraft," *Journal of Guidance, Control, and Dynamics*, Vol. 19, No. 4, 1996, pp. 954–960.

[11] Singhose, W., Singh, T., and Seering, W., "On–Off Control with Specified Fuel Usage," *Journal of Dynamic Systems, Measurement, and Control*, Vol. 121, No. 2, 1999, pp. 206–212.

[12] Souza, M. L. O., "Exactly Solving the Weighted Time/Fuel Optimal Control of an Undamped Harmonic Oscillator," *Journal of Guidance, Control, and Dynamics*, Vol. 11, No. 6, 1988, pp. 488–494.

[13] Wie, B., Sinha, R., Sunkel, J., and Cox, K., "Robust Fuel- and Time-Optimal Control of Uncertain Flexible Space Structures," *Proceedings of Guidance, Navigation, and Control Conference*, AIAA, Monterey, CA, 1993, pp. 939–948.

[14] Singh, T., "Fuel/Time Optimal Control of the Benchmark Problem," *Journal of Guidance, Control, and Dynamics*, Vol. 18, No. 6, 1995, pp. 1225–1231.

[15] Singer, N. C., and Seering, W. P., "Preshaping Command Inputs to Reduce System Vibration," *Journal of Dynamic Systems, Measurement, and Control*, Vol. 112, March 1990, pp. 76–82.

[16] Singhose, W., Derezinski, S., and Singer, N., "Extra-Insensitive Input Shapers for Controlling Flexible Spacecraft," *Journal of Guidance, Control, and Dynamics*, Vol. 19, No. 2, 1996, pp. 385–91.

[17] Singhose, W., Banerjee, A., and Seering, W., "Slewing Flexible Spacecraft with Deflection-Limiting Input Shaping," *Journal of Guidance, Control, and Dynamics*, Vol. 20, No. 2, 1997, pp. 291–298.

[18] Singhose, W., Mills, B., and Seering, W., "Closed-Form Methods for Generating On–Off Commands for Undamped Flexible Structures," *Journal of Guidance, Control, and Dynamics*, Vol. 22, No. 2, 1999, pp. 378–82.

[19] Singhose, W., Biediger, E., Okada, H., and Matunaga, S., "Closed-Form Specified-Fuel Commands for On–Off Thrusters," *Journal of Guidance, Control, and Dynamics*, Vol. 29, No. 3, 2006, pp. 606–611.